NUMERICAL AND EXPERIMENTAL STUDY OF A FREE INCOMPRESSIBLE ISOTHERMAL TURBULENT COAXIAL JET

G. R. Ströher[a], C. A. Martins[b], and C. R. de Andrade[b]

[a] Universidade Tecnológica Federal do Paraná
Coordenação de Processos Químicos
R. Marcílio Dias, 635
CEP. 86.812-460, Apucarana, Paraná, Brasil

[b]Instituto Tecnológico de Aeronáutica
Departmento de Engenharia Aeronáutica
Pr. Marechal Eduardo Gomes, 50
CEP 12.228-900, São José dos Campos,
São Paulo, Brasil.

*Corresponding author: Gylles Ricardo Ströher
gylles@utfpr.edu.br

ABSTRACT

In the present study the free incompressible isothermal turbulent coaxial jet problem is numerically solved, and compared with experimental measurements for different velocity ratio between the inner and the outer streams of the jet. The radial profile of the axial mean velocity was obtained with hot anemometry at different axial positions. Governing equations (mass conservation, momentum, turbulence model) were discretized employing the finite volume method with a segregated solver. The analysis of the experimental results showed that coaxial jet flow fields did not present self-similarity up to z/D=25, and the numerical solution using the Shih's k ε turbulence model did not match reasonably with the experimental data, with a difference of about ± 10%.

Keywords: Coaxial Jet, Anemometry Measurements, Turbulence Modeling.

NOMENCLATURE

V	Reynolds-averaged velocity vector, m s^{-1}
D	pipe diameter, m
A	area, m2
Re	Reynolds Number
Vi	Reynolds averaged axial velocity, m s^{-1}
Vj	Reynolds averaged radial velocity, m s^{-1}
Pk	turbulence production term , kg m^{-1} s^{-3}
P	Reynolds-averaged pressure, Pa
$C_{1\varepsilon}$	turbulence model constant
$C_{2\varepsilon}$	turbulence model Constant
σ_k	turbulence model Constant
σ_ε	turbulence model constant
K2	spreading rate
z_{o2}	virtual origin, m
r	radial coordinate, m
z	axial coordinate, m
$r_{1/2}$	haf-radius, m
S_{ij}	Mean strain rate tensor, s^{-1}

Greek symbols

ρ	density, kg/m3
μ	dynamic molecular viscosity, N s m^{-2}
μ_t	eddy viscosity, N s m^{-2}
ε	turbulence dissipation rate, m^2 s^{-3}
λ	velocity ratio
α	thermal diffusivity, m^2/s
ρ	density, kg/m^3
τ	dimensionless time

Subscripts

i	inner pipe
o	annular section
0	exit of the pipe

INTRODUCTION

Coaxial turbulent jets issuing from two round coaxial nozzles can be found in a great assortment of engineering applications. This system represent a flow field that provides one of the simplest cases of a wide range of problems involving the interaction or mixing between turbulent shear flows (e.g. combustion chambers, mixing tanks, cooling systems, and premixed burners).

Two or three zones are often distinguished in the coaxial jets, as shown in Fig.1. The initial mixing region of the jet corresponds to the development of mixing layers between fluids: an inner mixing layer between the inner fluid and the outer fluid, and an outer mixing layer between the outer fluid and the environment. Far from the nozzle (several tens inner diameters away), the structure of the double jet is the same as that of a simple jet (Ablitzer et al. 2002). This region is characterized by self-similar profiles, this means that the profiles of a flow quantity, such as the axial mean velocity, taken at different downstream distances, will all collapse when properly scaled (Pope 2000). Furthermore, the transition zone between initial and fully-merged zone regions has been scarcely studied.

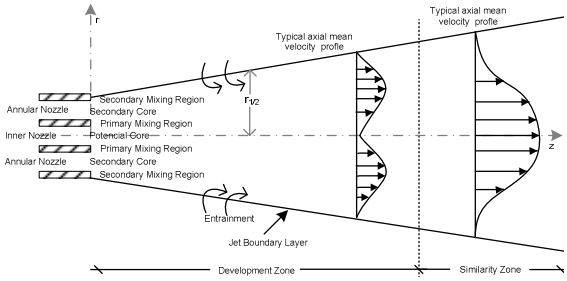

Figure 1. Schematic of a Coaxial turbulent jets issuing from two round coaxial nozzles.

Similarity, also called self-preservation, is a very interesting feature of flows, in this the flow properties depend on one variable only. Due to the large number of old experimental studies in the similarity region, a hypothesis was established in the past that a turbulence "forget" its origins, in the case that the flow can be considered two-dimensional or axisymmetric. Further information about similarity and turbulent jet flows can be obtained in George (1989) and George and Davidson (2004).

Several investigations have documented through hot-wire measurements the influence of the operating conditions of the coaxial turbulent jets on the general characteristics of the mean and of fluctuation flow fields. In agreement with Celik and Eren (2009) the main factor affecting the coaxial jet flow is the velocity ratio λ ($\lambda = Vz_i/Vz_0$, where Vz_i is the mean axial velocity at the exit of the inner pipe, and U_0 is the mean axial velocity at the exit of annular section).

Durao and Whitelaw (1973) investigated the developing region of coaxial jets at downstream distances up to 17 outer diameters. The measurements were obtained for three velocity ratios Vz_i/Vz_0 of 0.62, 0.23, and 0.0. Their results showed that coaxial jets tend to reach a self-preserving state much more rapidly than axisymmetric single jets.

Champagne and Wygnanski (1971) used a hot-wire anemometer to evaluate coaxial turbulent jets. Their observations were made at two area ratios A_o/A_i = 0.94 and 1.28 with the corresponding Reynolds numbers ranging from 0.0 to about 10^5 for both jets. The velocity ratio variation was $0.0 \leq Vz_o/Vz_i \leq 10.0$. The internal jet was never completely stopped to prevent the creation of an angular jet with its low-pressure recirculating bubble through which the hot wire can not function properly as it can not distinguish the reversed flow.

Different aspects of coaxial jet flows have been experimentally studied by many researchers, as abovementioned. Not differently, a significant progress, especially concerning the turbulence modeling, has been made to understand the jet exit effects on flow dynamics. Many investigations were performed using different Rans turbulence models for single free jet, however, results from the application the Rans models are scarce for coaxial turbulent jets. Among the RANS turbulence models of the two equations, the k-ε turbulence model from Shih et al. (1995), (also known as "realizable" k-ε) has presented good agreement with experimental data for single free jet when the flow is incompressible in the nozzle. Once far from the nozzle, the coaxial flow structure becomes the same as that of a simple jet, so the Shih's model is a good attempt for the coaxial jet flow.

In order to analyze the flow characteristics of the coaxial jet from different velocity ratio λ, various axial and radial velocity profiles were measured using a hot wire anemometer for the incompressible flow regime. Additionally the experimental data were compared with numerical results obtained with the turbulence model from Shih et al. (1995).

EXPERIMENTS

From simple to complex techniques, including laser light, there are several methods to obtain experimental velocity measurements. Here, it was employed the anemometry technique. Anemometry is an indirect measuring technique, i.e., requires calibration in a known flow field before its appliance to measure the fluid flow velocity. The wire of a typical HWA has 5 μm diameter and temperature from 150 to 300 °C during operation. The correlation between the flow velocity and heat transfer rate has been approached mainly empirically, and the form of the calibration equations was derived from a large number of experiments (Lange et al. 1999). Hot wire anemometer utilized in present work has uncertainty of 3% considering a 95 % confidence interval. The experimental set-up used to obtain the velocity field is presented in Fig. 2a.

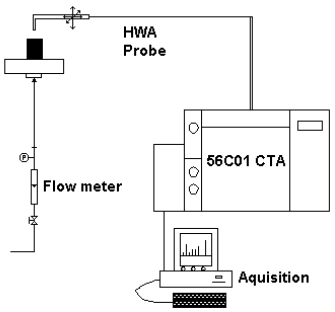

(a)

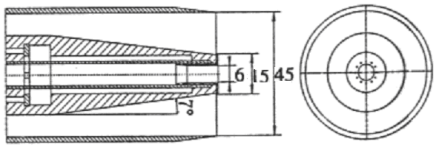

(b)

Figure 2. (a) Schematic representation of the HWA configuration. (b) Configuration of the nozzle.

Primarily the studied configuration is utilized how burner more specific natural gas burner. Herein it was assessed an isothermal main jet of air with a primary air flow. This consists of a round fuel tube and an annulus for primary air supply. Primary air issues from a rather narrow annulus so this air flow also has the character of a jet and turbulent mixing of fuel (main jet) and air is enhanced. Schematic configuration is shown in Fig. 2b.

Measurements in isothermal jets have been obtained under the conditions presented in Table 1, where are given the respective means velocity of exit and Reynolds numbers in the jet inner and annulus section. The case V is a typical single free jet flow.

Table 1. Flow settings for the isothermal jets.

	Inner Section		Annulus Section		
Case	Vz_i (m/s)	Re_{i0}	Vz_o (m/s)	Re_{o0}	λ
I	20.0	7561	4.4	8317	4.54
II	20.0	7561	7.3	13799	2.74
III	11.1	4196	4.3	8128	2.58
IV	14.3	5406	5.0	9451	2.86
V	20.0	7561	-	-	-

NUMERICAL SIMULATION

The system in the present study is an coaxial air jet emerging into an surrounding initially stagnant air. The coordinate system, computational domain and boundary conditions are plotted in Fig. 3. The flow field of coaxial jets was solved as a two-dimensional axisymmetric flow, using the finite volume method. To eliminate the effects of the exit boundary conditions on the flow, the L_{out} and H_{out} of the simulation domain were expanded to $60D_o$ and $10D_o$, respectively, L_t = 1.0m. Outlet boundary applied constant pressure outlet equal to standard atmospheric pressure (101,325 Pa), so gauge pressure was set to 0, and the inlet velocity was set using the law of conservation of mass and the values from the Tab. 1.

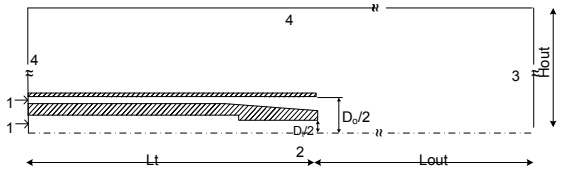

Figure 3. Solution domain and boundary conditions (drawing without scale). 1: inlet uniform velocity plane $v_r = 0$, v_z = constant inflow; 2: axis of symmetry $\nabla p \bullet \vec{n} = 0$, $\nabla v_z \bullet \vec{n} = 0$ e $v_r = v_\theta = 0$; (3): uniform static pressure $p_s = p_{amb}$ at outlet cells; (4): uniform total pressure $p_t = p_{amb}$ for incoming flow (entrained flow)

The flow field was considered incompressible, stead steady, axisymmetric and turbulent. The governing Reynolds-averaged transport (RANS) equations can be given in the following way:

Continuity equation:

$$\nabla \cdot V = 0 \tag{1}$$

Momentum equation:

$$V \cdot \nabla V = -(1/\rho)\left[\nabla P + \nabla \cdot \left[\left(\mu + \mu_t\right)\nabla V\right]\right] \tag{2}$$

where ρ is the density, V is the Reynolds-averaged velocity vector, P is the Reynolds-averaged pressure, μ is the dynamic molecular viscosity, and μ_t is the eddy viscosity.

In order that the mean flow equations can be closed, the eddy viscosity μ_t was computed using the realizable k-ε. Between the two equations of Reynolds Average Navier–Stokes (RANS) turbulence models, realizable k-ε is known as the most suitable for a round single jet, Shih et al. (1995). In this model, the eddy viscosity is computed using the relationship:

$$\mu_t = \rho C_\mu \frac{k^2}{\varepsilon} \tag{3}$$

The values of k and the dissipation, ε, were resulted from the solution of the transport equations. The k-equation (Eq. 4) is derived by subtracting the instantaneous mechanical energy from its time averaged value, and for the ε-equation (Eq. 5) Shih et al. (1995) proposed a new model dissipation rate equation, based on the dynamic equation of the mean-square vorticity fluctuation at large turbulent Reynolds number, and C_μ is computed from Eq.(7):

$$\rho V_i \frac{\partial k}{\partial x_i} = \frac{\partial}{\partial x_i}\left(\mu + \frac{\mu_t}{\sigma_k}\right)\frac{\partial k}{\partial x_i} + P_k - \rho\varepsilon \quad (4)$$

$$\rho V_i \frac{\partial \varepsilon}{\partial x_i} = \frac{\partial}{\partial x_i}\left(\mu + \frac{\mu_t}{\sigma_k}\right)\frac{\partial \varepsilon}{\partial x_i} + \rho C_1 S_\varepsilon - \rho C_2 \frac{\varepsilon^2}{k+\sqrt{v\varepsilon}} S_\varepsilon \frac{\varepsilon}{k}\left(C_{\varepsilon 1} P_k - C_{\varepsilon 2}\rho\varepsilon\right) \quad (5)$$

The turbulence production term, Pk, is modeled using:

$$P_k = \mu_t \frac{\partial V_i}{\partial x_i}\left(\frac{\partial V_i}{\partial x_i} + \frac{\partial V_j}{\partial x_i}\right) \quad (6)$$

The values for the standard *k*-ε equation constants used in this study are C_μ = 0.09, $C_{\varepsilon 1}$ = 1.45, $C_{\varepsilon 2}$ =1.9, σ_k =1.0, and σ_ε =1.3.

In the realizable *k*-ε model, the eddy viscosity is computed as the standard *k*-ε model, but C_μ is not constant. It is computed from:

$$C_\mu = \frac{1}{A_0 + A_S \dfrac{kU^\bullet}{\varepsilon}} \quad (7)$$

where

$$U^\bullet \equiv \sqrt{S_{ij}S_{ij} + \tilde{\Omega}_{ij}\tilde{\Omega}_{ij}}\,, \quad \Omega_{ij} = \overline{\Omega_{ij}} - \varepsilon_{ijk}\omega_k \quad (8)$$

where $\overline{\Omega_{ij}}$ is the mean rate-of-rotation tensor viewed in a rotating reference frame with the angular velocity ω_k .The model constants are $A_0 = 4.04$, $A_s = 6^{0.5}\cos\phi$, where:

$$\phi = \frac{1}{3}\cos^{-1}\left(\sqrt{6}W\right), \quad W = \frac{S_{ij}S_{ik}S_{ki}}{\tilde{S}}, \quad \tilde{S} = \sqrt{S_{ij}S_{ij}}, \quad S_{ij} = \frac{1}{2}\left(\frac{\partial u_j}{\partial x_i} + \frac{\partial u_i}{\partial x_j}\right) \quad (9)$$

The values for the realizable *k*–ε equation constants used in this work were $C_{1\varepsilon} = 1.44$, $C_{2\varepsilon} = 1.9$, $\sigma_k = 1.0$ and $\sigma_\varepsilon = 1.2$.

SOLUTION STRATEGIES

The axisymmetric turbulent flow field was calculated by solving the Reynolds Averaged Navier-Stokes equations (RANS) and turbulence models equations available in a CFD package (FLUENT 6.3). The equations are discretized by finite volume method and solved using the "uncoupled" solver and convective terms discretized using the spatial second order scheme (Barth and Jespersen, 1989). The pressure-velocity coupling algorithm used was the SIMPLEC (Vandoormaal and Raithby, 1984). Solutions were considered converged when the maximum residual of all the discretized equations was lower than 1×10^{-5}, and when the total momentum in z direction remained constant and independent of the distance z from the nozzle.

Structured and uniform grids were generated for the solution domain shown in Fig. 3. Mesh independence tests were performed using three computational grids with the following cell numbers 30,000 (coarse), 60,000 (medium), and 100,000 (fine). The maximum differences in the centerline velocity (along the z axis) between the coarse and medium grids, and between the medium and the fine grids, were lower than 0.5% and 0.05%, respectively (within typical experimental error range). Based on these results, the medium grid showed in Fig. 4, not fully, was selected for all computations in the present investigation.

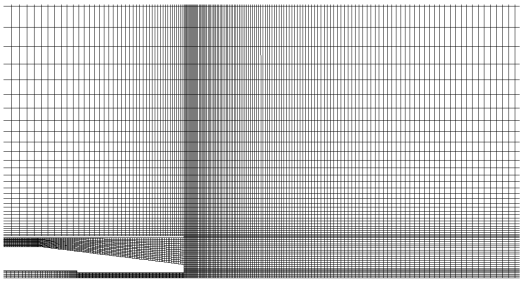

Figure 4. Detailed view of grid for exit nozzle.

RESULTS AND DISCUSSION

This section is organized into two parts: the first part comprises the experimental data obtained from hot-wire anemometry and the second part presents the numerical results.

Experimental Results

Figure 5 present the varying the velocity ratio λ, on the decay of mean longitudinal velocities along the jet centerline. The mean velocity decay does not suffer systematic variation with λ, and as expected, the mean velocity decays faster for the single jet, and since mean momentum rate of the single jet was lower than coaxial jets, the mean velocity decays faster for the single jet.

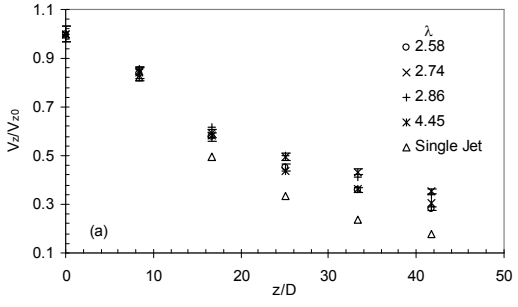

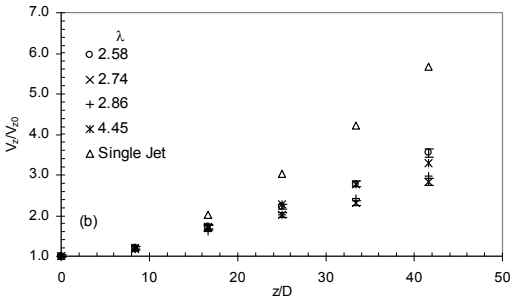

Figure 5. (a) The decay along the centerline of the axial mean velocity of a coaxial and a single jet. (b) the reciprocal of the decay along the centerline of the axial mean velocity of a coaxial jet and a single jet.

In order to examine the evolution of flow of different λ, the radial profiles of the mean and fluctuating velocities at different axial location are presented in Figs 6 and 7, respectively.

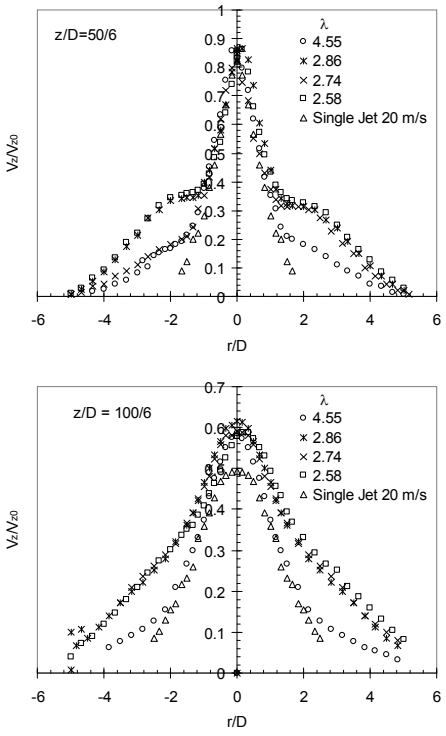

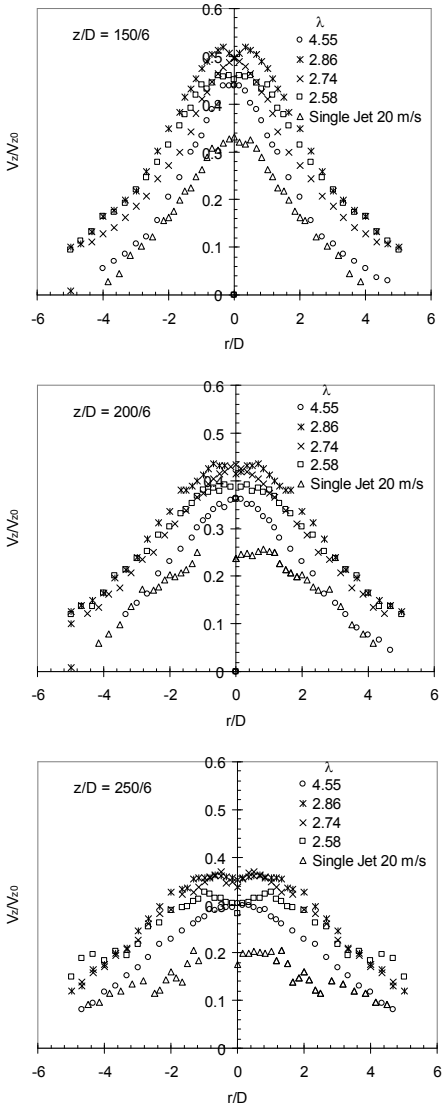

Figure 6. Radial profiles of the axial mean of a coaxial jet.

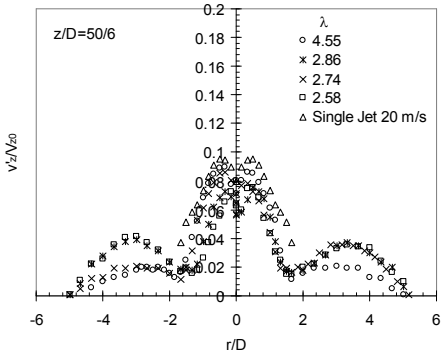

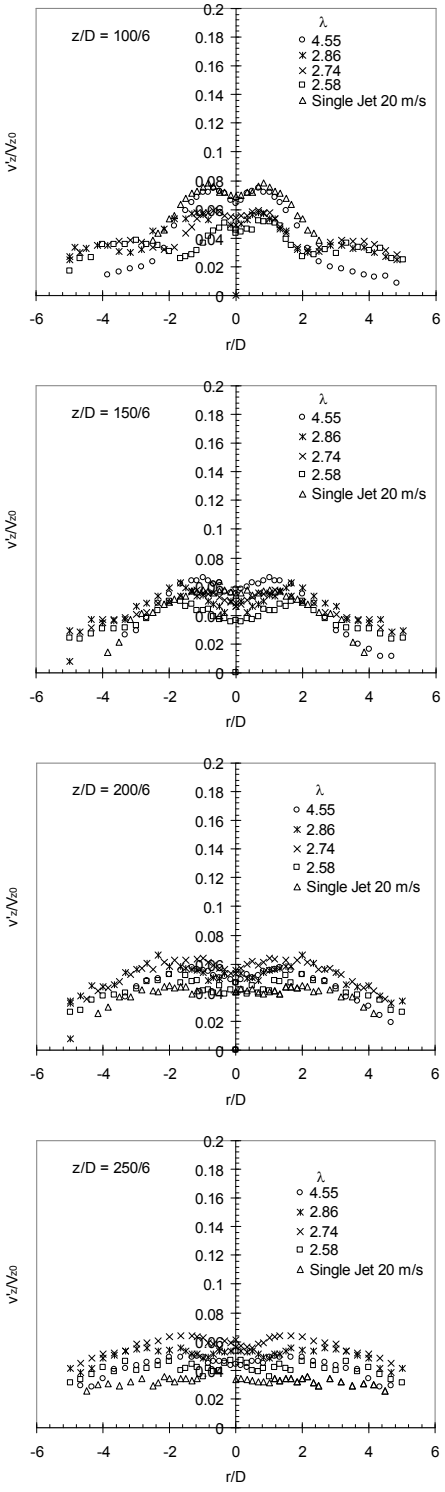

Figure 7. Radial profiles of the axial turbulence intensity of a coaxial jet.

The set profiles in Figs. 6 and 7 present almost complete symmetry, thus providing reliability for the hypothesis of symmetric flow for the numerical simulation with little effect on the numerical conclusions. In Fig. 6 it can be observed that near the nozzle, z/D=50/6, the case with greater velocity ratio have similar profile of the single jet. For the other cases the flow presents one secondary core zone that decreases due to the shear with the stagnated environment air (secondary mixing) and with inner jet (primary mixing). One can observe that the mean decay velocity is greater for the highest velocity ratio and as expected, the mean velocity from single jet is smaller than the coaxial flow.

As observed in Fig. 7, near the nozzle, the single jet presented the highest intensity turbulence. As the flow moves downstream, the turbulence intensity decreases until far from the nozzle, the jet presents the smallest value of turbulence intensity. Far from the nozzle, for the coaxial jets, there are loss of momentum among the inner and outer jet and the still environment air.

The similarity of the axial mean velocity profiles was investigated and compared with the results of the single jet from Schilichting (1979), thus, Fig. 8 was prepared to indicate the tendency of the coaxial jets to attain equilibrium velocity decay, in other words, to investigate the self-preserving condition. It is said to occur when the profiles of velocity (or any other quantity) can be brought into congruence by simple scale factors which depend on only one of the variables. A consequence of self-preservation is that the dynamical equations become independent of that variable, and are reduced by one variable in their functional dependence.

There are many alternative definitions for the dynamical significance of self preservation, however, in the classical sense self-similarity implies that the jet mixing field can be characterized using appropriate normalized parameters which depend on only one velocity (or a scalar quantity) and one length scale (e.g. Townsend 1976; Tennekes and Lumley 1972; Hinze 1976).

In cylindrical coordinates, the self-similar radial profiles of the mean velocity can be expressed as:

$$v_z = v_{z(r=0,z)}(z)\, f(\eta) \tag{10}$$

$$\eta = r/\delta \tag{11}$$

$$\delta = \delta(z) \tag{12}$$

The profile functions $f(\eta)$ account for all of the radial variation, and their existence implies that the profiles of velocity at every downstream location can be collapsed into single curves. All of the streamwise variation has been incorporated into the functions $v_{z(r=0,z)}$, and $\delta(z)$ which must be determined so that all terms in the dynamical equation maintain the same relative balance at the relative location. If such solutions are possible, an equilibrium between terms has been established and the flow evolves in a highly structured way. so the flow can be considered to be self-preserving. Several functions are used for $\delta(z)$, some examples can be seen in Mi et al. (2000) and George (1989), in this study it was used:

$$\delta(z) = r_{1/2}(z) = K2\,(z - z_{02}) \qquad (13)$$

where, $r_{1/2}$ is defined as the radial location at which the local mean scalar is equal to half its value at the centerline, i.e. $v_z(z,r_{1/2}) = 0.5\, v_{z(r=0,z)}$, $K2$ is the spreading rate of $r_{1/2}$, and z_{o2} is the virtual origin associated with the half-radius $r_{1/2}$.

For all the cases velocity ratios, similarity is not satisfactory in the development region and no agreement is confirmed even with the results of the single jet. Subsequently, about 150D/6 (25 D) good similarity is observed in the fully merged region, in other words, the profiles collapsed into single curves. This result matches with those from Warda et al. (2001), for coaxial jets with λ = 2, 3,3 and 4,5 the flow fields did not show self-similarity up to z/D=25.

Furthermore, good agreement with the single jet results in the fully merged (developed) region was also found for only single jet case. For single jet case, the data was compared with typical profile available in several fundamental books of mechanics fluids, it can be used the example proposed for the profile from Schilchiting (1979). One can see that the profiles become self-similarity about after 150D/6 (25 D). This distance is larger than that found by Ferdman et al. (2000) for round jet with Re_0 = $2{,}4x10^4$ and axisymmetric and asymmetric initial velocity distribution, obtained after 15 D, the self-similarity mean velocity profiles of both jets. Rahman et al. (1997) for round jet and Re_0 =$1.32x10^4$, $2.64x10^4$ and $3.96x10^4$, obtained self-similarity mean velocity profiles after 8 D.

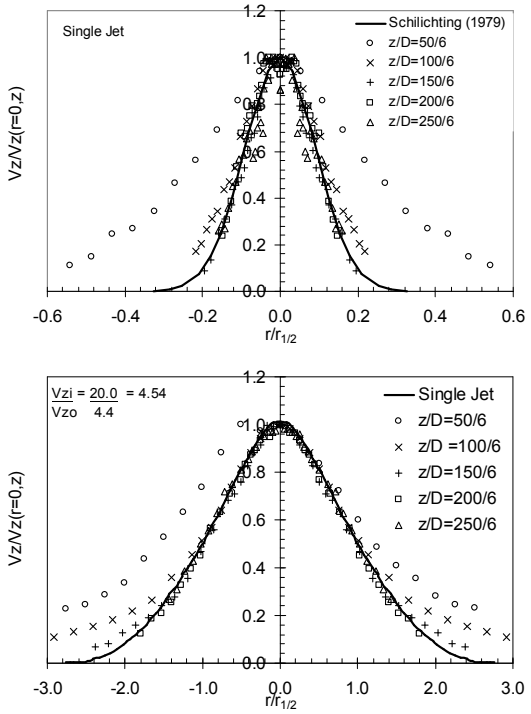

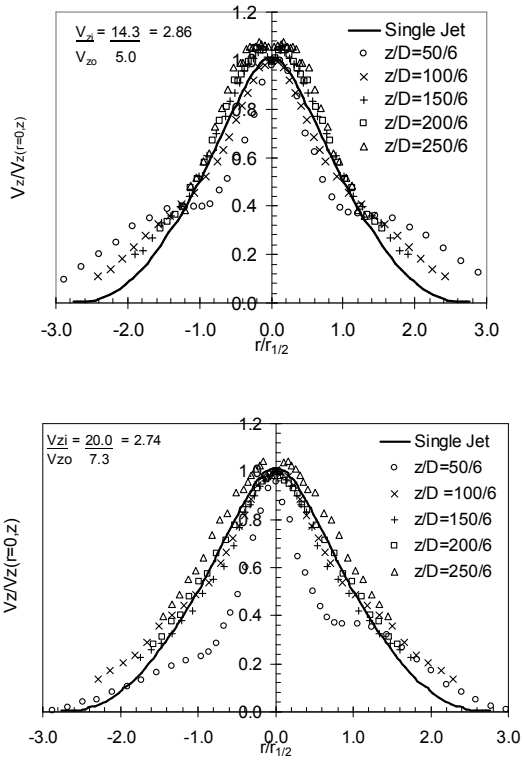

Figure 8. Similarity study.

Numerical Results

In the numerical approach, the turbulence model from Shih et al. (1995) was used to investigate the capability of this model to predict the coaxial jets flow field. According to Shih et al. (1995) for incompressible round jet this model predicted better results than various versions of k–ε models. However, there is not many information available about this model for coaxial jets. The cases I to IV was simulated with the sets commented in section 3 and the results are showed in Fig. 9, where (a) presents both the profiles experimental and numerical of the axial mean velocity at different axial location, and (b) presents how much the numerical axial mean velocity deviated from the experimental, for example, if a numerical results fully agreed with experimental data, a curve as the identity function (f (x) = x) would be obtained (Fig.9 b, dashed line). Notice that Fig. 9 (b) was set only with data from Fig. 9 (a) to r/D ≥ 0.

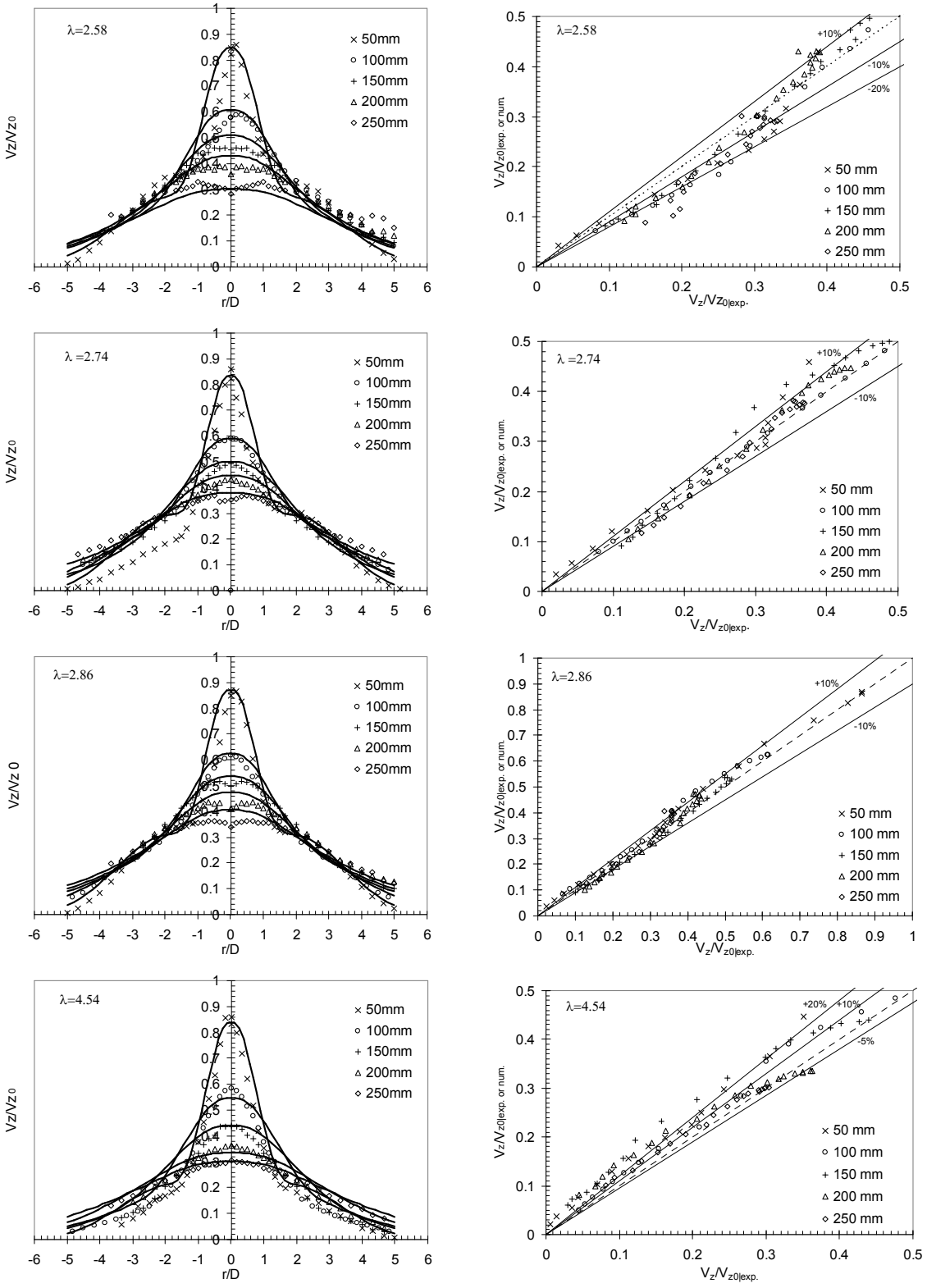

(a) numerical (solid line), experimental (symbols)

(b) numerical (symbols), experimental (dashed line) deviate from experimental (solid line)

Figure 9. Comparison between experimental and numerical profiles for the mean axial velocity.

As can be seen in Fig. 9, the numerical data did not match reasonably with the experimental data with a difference about of ± 10%, greater than the experimental uncertainty. The higher differences were found for the extremity cases of velocity ratio, λ =4.54 and 2.58, and for the lower velocity values. For λ =4.54, the simulation predicted values above the experimental ones, in particular for stations 150 and 200 mm (over + 20%) and r/D> 1.5. Whilst, for λ =2.58 the simulation underestimates (over - 20%). This result may indicate that the turbulence model tested did not preserve its predicting as good as for single jet flow. The main difference between single and coaxial free jet flow field is that the single jet presents only one potential core and mixing regions, and thus the jet exchanges momentum only with the stagnant environment fluid, whereas for coaxial jets there are primary and secondary potential and mixing regions and the exchange of momentum between these regions can not be adequately provided by the Shih's turbulence model. However, other factors can explain the disagreement between experimental and numerical data as boundary conditions and experimental and numerical methodologies, so that, further cases must be simulated to evidence this weakness of the Shih turbulence model.

CONCLUSIONS

In the present study, the axisymmetric coaxial incompressible isothermal turbulent free jet problem was numerically solved and compared with experimental measurements obtained with hot anemometry at different axial positions. The measurements and numerical results obtained, presented and discussed allowed the following conclusions: (a) the decay of mean longitudinal velocities along the jet centerline and the radial profiles of the mean and fluctuating velocities depends on the velocity ratio, (b) the similarity of the radial profiles of the axial mean velocity was obtained in the fully merged region of coaxial jets with different velocity ratio, (c) the coaxial jet flow fields did not show self-similarity up to z/D=25, and (d) in present simulations the Shih's k ε turbulence model did not match reasonably with the experimental data, with a difference of about ± 10%.

ACKNOWLEDGEMENTS

The authors are grateful to Fapesp (Fundação de Amparo à Pesquisa do Estado de São Paulo) for the support in experimental part of this work through Projects 98/15539-0.

REFERENCES

Ablitzer C., Gruy F., and, Perrais C., 2002, Influence of macromixing on powder formation in a reactive coaxial jet. Chemical Engineering Science, Vol. 57, p. 2837–2848.

Barth T. J., and Jespersen D., 1989, The design and application of upwind schemes on unstructured meshes. Technical Report AIAA-89-0366, AIAA 27th Aerospace Sciences Meeting, Reno, Nevada.

Berg, J. R., Ormiston S. J., and Soliman, H. M., 2006, Prediction of the Flow Structure in a Turbulent Rectangular Free Jet, International Communications in Heat and Mass Transfer, Vol. 33, pp. 552–563.

Celik, N., and Eren, H., 2009, Heat transfer due to impinging co-axial jets and the jets' fluid flow characteristics, Experimental Thermal and Fluid Science, Vol. 33, pp. 715–727.

Champagne, F. H., and Wygnanski, I. J., 1971, An experimental investigation of coaxial turbulent jets, Int. J. Heat and Mass Transfer, Vol. 14, pp. 1445–1464.

Durao, D., and Whitelaw , J. H., 1973, Turbulent Mixing in the Developing Region of Coaxial Jets, Trans ASME, J. Fluids Engng, Vol. 95, pp. 467–473.

Ferdman, E., Ötügen, M. V., and Kim S., 2000, Effect of Initial Velocity Profile on the Development of Round Jets, Journal of Propulsion and Power, Vol. 16, No. 4, pp. 552-561.

George, W. K., and Davidson, L., 2004, Role of Initial Conditions in Establishing Asymptotic Flow Behavior, AIAA Journal, Vol.47, pp. 438-446.

George, W. K., 1989, The Self-similarity of Turbulent Flows and its Relation to Initial Conditions and Coherent Structures, In Recent Advances in Turbulence (ed. R. E. A. Arndt & W. K. George), pp. 39-73.

Ghazi, M., and Olwi I. 1997, Experimental Investigation of Plane Jet Flowfield Characteristics, American Institute of Aeronautics and Astronautics, Inc. A97-31786, pp. 925-935.

Hinze, J. O., 1975, *Turbulence*, 2nd Edn. McGraw-Hill.

Lange, C. F, Durst, F., and Breuer, M., 1999, Wall Effects on Heat Losses from Hot Wires, International Journal of Heat and Fluid Flow, Vol. 20, pp:. 34-37.

Mi, J., Nobis, D. S., and Nathan, G., 2001, Influence of Jet Exit Conditions on the Passive Scalar Field of an Axisymmetric Free Jet, Journal of Fluid Mechanics, Vol. 432, pp. 91–125.

Miller, R. S., Madnia, C. K., and Givi, P., 1995, Numerical Simulation of Non-Circular Jets, Computers and Fluids,Vol. 24, pp. 1–25.

Schlichting, H., 1979, *Boundary – Layer Theory*, seventh ed., McGraw – Hill, New York, p. 700.

Shih, T. H., Liou, W. W., Shabbir, A., Yang Z., and Zhu, J. A., 1995, New k-ε Eddy-Viscosity Model for High Reynolds Number Turbulent Flows, Model Development and Validation, Computers Fluids, Vol. 24, No. 3, pp. 227-238.

Tennekes, H. and Lumley, J. L., 1972, *A First Course in Turbulence*, MIT Press.

Townsend, A. A., 1976, *The Structure of Turbulent Shear Flow*, 2nd edn. Cambridge University Press.

Vandoormaaland, J. P., and Raithby, G. D., 1984, Enhancements of the SIMPLE Method for Predicting Incompressible Fluid Flows, Numer. Heat Transfer, Vol. 7, pp. 147-163.

Warda, H. A., Kassab, S. Z., Elshorbagy, K. A., and Elsaadawy, E. A., 1999, An Experimental Investigation of the Near-field Region of a Free Turbulent Coaxial Jet Using LDA, Flow Measurement and Instrumentation, Vol. 10, pp. 15–26.

Warda, H. A., Kassab, S. Z., Elshorbagy, K. A., and Elsaadawy, E. A., 2001, A Influence of the Magnitude of the Two Initial Velocities on the flow field of a Coaxial Turbulent Jet, Flow Measurement and Instrumentation, Vol. 12, pp. 29–35.

Wilson, R. V., and Demuren A. O., 1996, Numerical Simulation of Turbulent Jets with Rectangular Cross-Section, ASME FED 238, pp. 121–127.

Received: January 15, 2010
Revised: February 15, 2010
Accepted: March 15, 2010